Applied Catalysis A, General 611 (2021) 117979

Contents lists available at ScienceDirect

Applied Catalysis A, General

journal homepage: www.elsevier.com/locate/apcata

Catalytic isomerization of dihydroxyacetone to lactic acid by heat treated zeolites

Md Anwar Hossain [a], Kyle N. Mills [a], Ashten M. Molley [a], Mohammad Shahinur Rahaman [a], Sarttrawut Tulaphol [a,b], Shashi B. Lalvani [c], Jie Dong [d], Mahendra K. Sunkara [a,e], Noppadon Sathitsuksanoh [a,*]

[a] Department of Chemical Engineering, University of Louisville, Louisville, KY, 40292, USA
[b] Sustainable Polymer & Innovative Composite Materials Research Group, Department of Chemistry, Faculty of Science, King Mongkut's University of Technology Thonburi, Bangkok, 10140, Thailand
[c] Department of Chemical, Paper, and Biomedical Engineering, Miami University, Oxford, OH, 45056, USA
[d] Department of Chemistry, Southern Illinois University Edwardsville, Edwardsville, IL, 62026, USA
[e] Conn Center for Renewable Energy Research, University of Louisville, Louisville, KY, 40292, USA

ARTICLE INFO

Keywords:
Lactic acid
Zeolites
Lewis acids
Dihydroxyacetone
Isomerization

ABSTRACT

Lactic acid can be prepared by isomerization of renewable dihydroxyacetone over acid catalysts. However, the activities of Lewis acid and Brønsted acid sites in dihydroxyacetone isomerization are poorly understood. We prepared catalysts by heat treatment of ZSM-5. The heat treated ZSM-5 exhibited a greater Lewis acid site density and enhanced selectivity toward lactic acid. Dihydroxyacetone dehydration to the intermediate pyruvaldehyde was readily formed at 140 °C without added catalysts. Lewis acid sites were needed to convert pyruvaldehyde to lactic acid. Moreover, the Lewis acid site density was consistent with the order of catalytic performance, which suggested that the Lewis acid sites were the active sites for pyruvaldehyde rehydration. Conversely, the Brønsted acid sites were key in formation of unwanted product from pyruvaldehyde. These findings highlight the potential use of commercial zeolites as adjustable solid Lewis acid catalysts in biomass conversion reactions in which Lewis acid sites are needed.

1. Introduction

Production of biofuels and bioproducts from lignocellulosic biomass has the potential to mitigate CO_2 emissions and contribute to a sustainable economy [1,2]. Lactic acid (LA, 2-hydroxypropanoic acid) is an important lignocellulose-derived precursor for the production of food, chemicals, cosmetics, pharmaceuticals, and biodegradable plastics [3]. A rising market for lactic acid is in the production of biodegradable poly (lactic acid) [4–6]. Poly(lactic acid) has many applications, such as in sutures apparel, carpet, and food containers [7]. Moreover, lactic acid can be used for the synthesis of green solvents (lactate esters) [8].

Lactic acid is currently produced by bacterial fermentation of sugars and/or glycerol as feedstocks. The advantage of fermentation is its high selectivity toward lactic acid. Its major drawback is slow kinetics; adequate yield can require up to 3–6 days [9,10]. The chemical pathway is a faster route to the production of LA using glucose, fructose, and glycerol as feedstocks. Glucose/fructose undergoes retro-aldol to dihydroxyacetone, whereas glycerol undergoes oxidation to dihydroxyacetone. It is generally accepted that dihydroxyacetone undergoes a cascade reaction of (1) dihydroxyacetone dehydration to pyruvaldehyde and (2) subsequent pyruvaldehyde hydration to lactic acid using acid catalysts (Scheme 1) [11,12].

Homogeneous catalysts, such as mineral acids (HCl, H_2SO_4, and H_3PO_4) [11,12] and Lewis acid salts ($AlCl_3$ and $CrCl_3$) [12,13] are active catalysts for dihydroxyacetone isomerization to lactic acid. However, homogeneous catalysts have the classic problem of requiring catalyst separation and product purification. Therefore, it is greatly desirable to develop highly selective solid acid catalysts for dihydroxyacetone isomerization to lactic acid. Zeolites are commonly used as solid acid catalysts in the chemical and petroleum industries [14–16]. Their heat stability, shape selectivity, and tunable acidity make zeolites versatile in many acid-catalyzed reactions, such as aromatization of alkenes [17–19], esterification [20–25], alkylation [26–28], and isomerization [26,29–31]. Among all zeolites studied for dihydroxyacetone

* Corresponding author.
E-mail address: n.sathitsuksanoh@louisville.edu (N. Sathitsuksanoh).

https://doi.org/10.1016/j.apcata.2020.117979
Received 26 October 2020; Received in revised form 11 December 2020; Accepted 18 December 2020

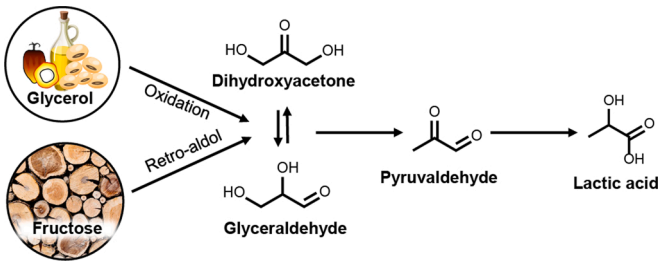

Scheme 1. Chemical pathway for lactic acid production.

isomerization to lactic acid, Sn-containing zeolites showed higher selectivity toward lactic acid [32–34]. However, despite their high selectivity, the commercial-scale production of Sn-containing β-zeolites is challenging because of a complicated synthesis procedure; this condition has slowed adoption of Sn-containing β-zeolites in industrial applications [35]. Clearly, industry needs additional simple, yet efficient, heterogeneous catalysts with high lactic acid selectivity.

Investigators have found that heat treatment of zeolites enhanced the activity of their Lewis acids (LAS) and improved paraffin conversion [36], hexane conversion [37], and methane aromatization [38]. The major reason for activity enhancement was the formation of extra-framework aluminum (EFAL) species by dehydroxylation of the Brønsted acid sites (BAS) of the parental zeolites [39]. These aluminum species of EFAL occur in various forms, such as Al^{3+}, $Al(OH)_2^+$, $Al(OH)^{2+}$, $Al(OH)_2$, AlO(OH) and Al_2O_3, exhibiting the Lewis acid sites (LAS) [39,40]. Heat treatment to generate LAS within zeolites is commercially accessible. However, there is poor understanding of the function of LAS generated from heat treatment and BAS of zeolites for DHA isomerization to LA in water.

Here we show the tunable LAS density of heat treated ZSM-5 catalysts (15 Si/Al ratio) and their activity in dihydroxyacetone isomerization to lactic acid in water. Heat treatment of ZSM-5 in the range of 700−900 °C created EFAL with Al^{3+} Lewis acid sites. The generation of LAS was confirmed by X-ray diffraction, Fourier Transform Infrared Spectroscopy, N_2 adsorption/desorption, and Diffuse Reflectance Infrared Fourier Transform Spectroscopy with adsorbed pyridine. The enhancement in lactic acid selectivity by high-temperature treatment of ZSM-5 implied that the LAS were responsible for the dihydroxyacetone isomerization to lactic acid.

2. Material and Methods

2.1. Materials

All chemicals were used as received unless otherwise noted. Their CAS numbers, purity, and manufacturers are listed in **Table S1**. ZSM-5 (15 Si/Al ratio) was obtained from Zeolyst® International (Conshohocken, PA, USA).

2.2. Catalyst preparation

The modified catalysts were prepared by heating ZSM-5 in air at 500, 700, and 900 °C in a tube furnace. In short, the ZSM-5 samples were placed in the ceramic boat. The temperature was raised at a rate of 5 °C/min and held isothermally for 10 h [41]. The samples were cooled to ambient temperature and stored in a desiccator. The heat treated ZSM-5 catalysts at 500, 700, and 900 °C were referred to as Z-500, Z-700 and Z-900. The Z-900 catalyst was washed with 0.1 M HCl at 65 °C for 6 h to remove the extra framework alumina [35]. The acid-washed sample was denoted as Z-900-AW.

2.3. Dihydroxyacetone isomerization to lactic acid and product analysis

Dihydroxyacetone isomerization was performed in 15 mL glass vials in an oil bath. In short, ~60 mg dihydroxyacetone (0.67 mmol) was dissolved in 4 mL deionized water. Approximately 20 mg catalyst was added to the pressure vial, which was sealed and stirred at 140 °C for varying reaction times. The reaction product was analyzed with an Agilent High-Pressure Liquid Chromatography (HPLC, Santa Clara, CA, USA) equipped with a diode-array detector (DAD) and refractive index detector (RID). The reactants, intermediates, and products were separated by a Bio-rad® Aminex 87H column with 4 mM H_2SO_4 as the mobile phase. The dihydroxyacetone conversion, product yield, and product selectivity were calculated as follows:

$$\text{Dihydroxyacetone conversion}(\%) = \frac{\text{Dihydroxyacetone reacted (mol)}}{\text{Initial dihydroxyacetone (mol)}} \times 100$$

$$\text{Product yield}\ (\%) = \frac{\text{Product formed (mol)}}{\text{Initial dihydroxyacetone (mol)}} \times 100$$

$$\text{Product selectivity}\ (\%) = \frac{\text{Product yield}\ (\%)}{\text{Dihydroxyacetone conversion}\ (\%)} \times 100$$

2.4. Characterization of catalysts

Infrared spectra of the zeolites were recorded on a JASCO-4700 Fourier transform infrared (FTIR) spectrometer (Easton, MD, USA), equipped with an attenuated total reflection stage (ATR, Pike Technologies, Madison, WI, USA). The surface area and pore volume of zeolites were measured using N_2 adsorption/desorption by a Tristar Micromeritics (Norcross, GA, USA) instrument. Prior to the measurement, the samples were pretreated at 160 °C for 2 h with a Micromeritics FlowPrep and sample degasser. The surface area and pore volume of catalysts were determined by N_2 adsorption/desorption using the Brunauer–Emmett–Teller (BET) [42] and Barrett–Joyner–Halenda (BJH) equations [43]. X-ray diffraction (XRD) analysis of samples was conducted on a Bruker D8 Discover diffractometer (Billerica, MA, USA) using CuK_α radiation and 2θ ranging from 10° to 60° with 0.2 s/step and 0.02°/step. The Brønsted acid site (BAS) density of the catalysts was quantified by temperature-programmed desorption-thermal gravimetric analysis (TPD-TGA) using n-propylamine as a probe molecule [44]. In short, catalysts were exposed to saturated n-propylamine at 50 °C for 12 h. The resulting samples were pretreated at 100 °C for 1 h under N_2 flow (100 cc/min) to remove the physisorbed n-propylamine. Then, the temperature was increased at a rate of 10 °C/min to a maximum of 500 °C.

To examine the acid properties, Diffuse Reflectance Infrared Fourier Transform Spectroscopy (DRIFTS) with adsorbed pyridine was performed on all catalysts using the JASCO-4700 FTIR spectrometer, equipped with a PIKE DiffuseIR® cell. In short, all samples were first dehydrated at 150 °C for 4 h to remove physisorbed water. Approximately 5 mg catalysts were positioned in the aluminum sample cup and exposed to saturated pyridine vapors by flowing 50 cc/min N_2 for 30 min. Then, the physisorbed pyridine was removed at 150 °C under N_2 for 30 min. The samples were heated under 50 cc/min N_2. The DRIFT spectra were recorded with a resolution of 4 cm^{-1} from 4000 − 1000 cm^{-1} for 256 scans. The DRIFT spectra of adsorbed pyridine showed three distinct bands between 1600−1400 cm^{-1}. The DRIFT bands at 1545 and 1445 cm^{-1} were assigned to the pyridine coordinated with Brønsted and Lewis acid sites, respectively [41,45]. The Lewis acid/Brønsted acid (LAS/BAS) ratio was determined from the ratio of intensities (integrals of peak areas) of the DRIFT bands at 1450 and 1545 cm^{-1} [46].

Spent catalysts were analyzed by thermogravimetric analysis (TGA) under N_2 flow (100 cc/min) ramping from 50 to 700 °C. TGA and

differential TGA profiles were used to determine the weight loss of catalysts. Weight loss up to 250 °C was attributed to physisorbed water, and the weight loss between 250−700 °C was attributed to the carbonaceous coke on the spent catalysts [47].

3. Results & discussion

3.1. Results

We studied the effect of heat treatment of ZSM-5 zeolites (Si/Al = 15) for dihydroxyacetone (DHA) isomerization to lactic acid in a batch reactor. We performed heat pretreatment of ZSM-5 at 500, 700 and 900 °C. We refer to the treated zeolites as Z-500, Z-700, and Z-900. We selected ZSM-5 with a Si/Al ratio of 15 because it had moderate acid sites, which made it possible to observe changes in acid sites after heat treatment. Then, we characterized the zeolites for changes in chemical structure and acidity, and we determined how the changes affected dihydroxyacetone isomerization to lactic acid.

3.2. Changes in chemical structure and acid properties of ZSM-5 catalysts after heat treatment

To measure the effects of heat treatment on the chemical structure of ZSM-5 catalysts, first, we characterized ZSM-5 by XRD and FTIR. The major XRD peaks of all ZSM-5 catalysts were similar and consistent with reported spectra [41,48]. Thus, the crystal structure of ZSM-5 was preserved after heat treatment (**Fig. S1**). An increase in treatment temperature from 500 to 900 °C caused a right-shift of (051) peak (2θ = 23.1°) (Fig. 1A). This shift of (051) peak with increasing temperature indicated a shortening of Si-O-Si bond length and contraction of the unit cells due to the reversible monoclinic to orthorhombic phase transition [49]. We further characterized these catalysts by FTIR to confirm the shortening of Si-O-Si bond length. One of the characteristic peaks of the ZSM-5 is its 1055 cm^{-1} band, assigned to the internal vibration of Si, AlO_4 tetrahedra (Fig. 1B). Following heat treatment, the internal vibration peak shifted toward the higher wavenumber because of an increase in Si-O bonds in relation to Al-O bonds [50]. The up-shift of 1050 cm^{-1} band corroborated our XRD results.

Next, we performed N_2 adsorption/desorption on our catalysts to quantify changes in surface area and pore volume after heat treatments. We calculated BET surface area and BJH pore volume from the N_2 adsorption/desorption isotherms (**Fig. S2**). The surface area and pore volume of the heat-treated catalysts increased slightly with increasing temperature (Table 1).

To examine changes in acid site type and density due to the heat treatment, we performed TPD-TGA with adsorbed n-propylamine and DRIFTS with adsorbed pyridine on our catalysts. TPD-TGA profiles of heat-treated zeolites showed a progressive decrease in the strong acid site (>250 °C). We calculated the BAS density. The Z-500 catalyst had

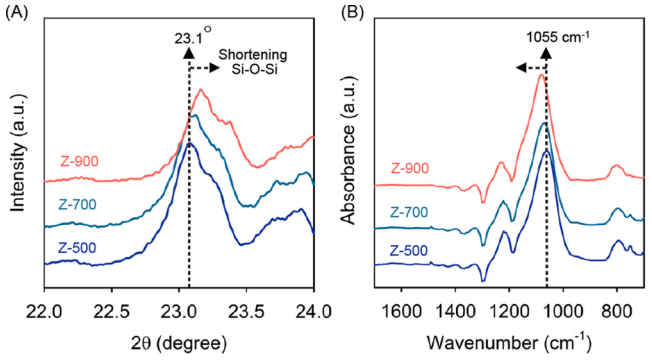

Fig. 1. XRD (A) and FTIR (B) spectra of modified ZSM-5 at different treatment temperatures.

0.55 mmol amine/g catalyst, in agreement with the reported value [51]. The BAS of the modified catalysts decreased with increasing temperature (Table 1). The DRIFT spectra of adsorbed pyridine enabled determination of LAS/BAS ratio (**Fig. S3B and** Table 1). An increase in temperature increased LAS/BAS ratio. We observed a slight increase in LAS. Hoff et al. showed that an increase in temperature of ZSM-5 from 550 to 900 °C decreased BAS by 4.0-fold and increased LAS/BAS ratio by 2.5-fold. In theory, zeolites have both BAS and LAS. BAS are derived from the hydrogen atoms of the zeolite framework [52]. Upon heat treatment, the zeolite framework undergoes dehydroxylation, which generates extra framework aluminum (EFAL). The resulting EFAL species are in various forms, such as oxoaluminum cations (AlO^+, $Al(OH)_2^+$, and $AlOH^{2+}$), neutral species (AlOOH and $Al(OH)_3$), and/or alumina cluster inside the supercage zeolites [53]. As a result, the BAS of the zeolites after heat treatment decreased and the LAS/BAS ratio increased. These results corroborated our findings and suggested that we could increase LAS density by heat treatment. As measured by TPD-TGA, we determined that an increase in treatment temperature caused a slight increase in LAS. In sum, the heat treatment generated the Lewis acid sites in the form of EFAL and decreased the Brønsted acid sites.

3.3. Catalytic performance of the heat treated ZSM-5 on the dihydroxyacetone isomerization

To examine the performance of the modified catalysts, we performed dihydroxyacetone isomerization at 140 °C. Dihydroxyacetone conversion progressively increased over time and reached >90 % by 6 h in all cases (Fig. 2A). Pyruvaldehyde and lactic acid were major products of this reaction. We observed a small amount of glyceraldehyde in the presence of catalysts, which suggested that dihydroxyacetone isomerization to glyceraldehyde occurred in the presence of these catalysts. As a control, the blank experiment (no added catalyst) showed that dihydroxyacetone conversion increased over time and reached >90 % by 6 h. We observed a gradual increase in pyruvaldehyde yield with a maximum of 32 % by 6 h. However, we did not observe lactic acid in the blank. Takagaki et al. [54] also showed that, in the absence of catalysts, dihydroxyacetone was converted to pyruvaldehyde, a finding that corroborates our observations.

Interestingly, with added catalysts, dihydroxyacetone conversion profiles were similar to the blank experiment. This phenomenon suggested that dihydroxyacetone conversion was a thermal reaction. With catalysts, the yield of PA increased and reached the maximum at about 2 h, then progressively decreased along with an increase in lactic acid yield. These results suggested that pyruvaldehyde was an intermediate product of dihydroxyacetone isomerization to lactic acid. This volcanic behavior of pyruvaldehyde over time was similar to the reported trend [55,56]. An increase in treatment temperature enhanced the selectivity of catalysts toward lactic acid. Z-900 had the highest lactic acid yield of 50 % after 6 h compared with 39 % for Z-700 and 21 % for Z-500. The increasing trend of lactic acid yield matched a corresponding increase in the LAS density of the catalysts (Table 1).

By plotting the yields of lactic acid and pyruvaldehyde with respect to LAS density, we observed that PA formation was relatively insensitive to the LAS density (Fig. 2B). However, an increase in LAS density enhanced the formation of lactic acid. We hypothesized that dihydroxyacetone dehydration was a thermal reaction. To test this hypothesis, we performed dihydroxyacetone isomerization in water at 90, 120, and 140 °C (**Fig. S4**). We observed pyruvaldehyde as the only reaction product. At 90 °C, the reaction mixture was clear, and we observed only a slight dihydroxyacetone conversion (<8%) after 6 h. At 120 °C, the pyruvaldehyde yield progressively increased and reached 29 % at 69 % dihydroxyacetone conversion (42 % pyruvaldehyde selectivity) after 6 h. Moreover, the reaction mixture was homogenous and light brown, which suggested formation of pyruvaldehyde (pyruvaldehyde is yellow/brown). Similarly, at 140 °C, the pyruvaldehyde yield increased over time and reached 43 % at 85 % dihydroxyacetone conversion (51 %

Table 1
Physical properties and acid densities of catalysts.

Catalyst	BET surface area (m^2/g)	Pore volume (cm^3/g)	Brønsted acid sites (BAS)[a] (μmol/g)	Lewis acid sites (LAS)[b] (μmol/g)	LAS/BAS[c]
Z-500	402	0.20	550	42	0.08
Z-700	464	0.25	410	56	0.14
Z-900	485	0.23	110	64	0.58
Z-900AW	488	0.27	60	3	0.05

[a] Measured by TGA-TPD with 2-propylamine.
[b] Calculated using BAS and LAS/BAS.
[c] Measured by DRIFTS with adsorbed pyridine.

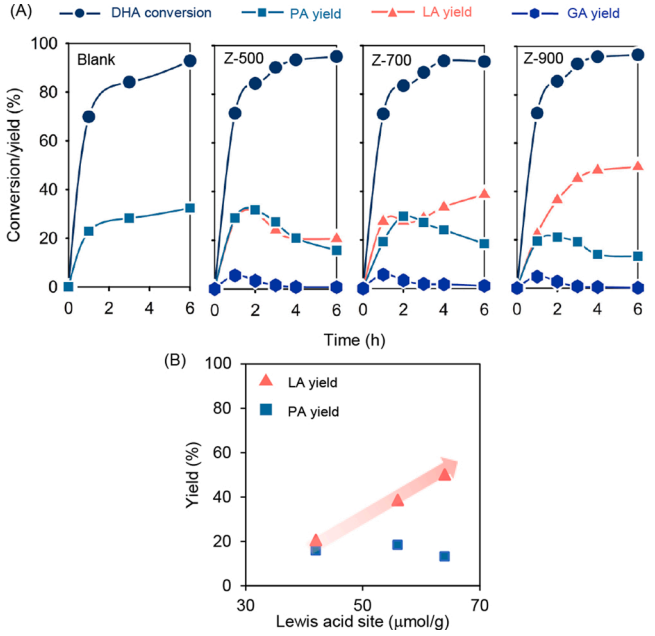

Fig. 2. Product evolution of the dihydroxyacetone isomerization by modified ZSM-5 (A). Relationship between yields of lactic acid and pyruvaldehyde at 6 h as a function of LAS density (B). *Reaction condition. 60 mg* dihydroxyacetone*, 20 mg catalyst, 4 g H_2O at 140 °C. DHA = dihydroxyacetone, GA = glyceraldehyde, PA = pyruvaldehyde, and LA = lactic acid.*

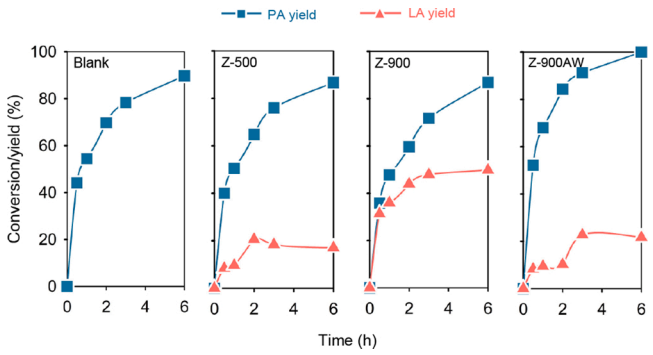

Fig. 3. Product evolution of pyruvaldehyde rehydration by modified ZSM-5. *Reaction condition. 60 mg pyruvaldehyde, 20 mg catalyst, 4 g H_2O at 140 °C.*

pyruvaldehyde selectivity) at 6 h. The reaction mixture became dark-brown, which suggested a higher amount of pyruvaldehyde formed compared with reaction at 120 °C. In addition, after 3 h, we observed black particles suspended in the reaction mixture, which indicated formation of coke (**Fig. S4 inset**). These results showed that dihydroxyacetone dehydration to pyruvaldehyde occurred more readily without added catalysts at temperature >120 °C. However, as the temperature rose to 140 °C, degradation of pyruvaldehyde became favorable. Our findings agreed with those of West et al. who observed that pyruvaldehyde degradation was favorable at high temperature (>115 °C) [57]. These results supported our hypothesis that the dihydroxyacetone dehydration to pyruvaldehyde was driven by the reaction temperature, and LAS was needed to convert pyruvaldehyde to lactic acid. In addition, our results suggested that LAS were active sites for pyruvaldehyde rehydration, in agreement with previous studies [58,59].

3.4. Pyruvaldehyde rehydration by heat treated ZSM-5

To decouple the activities of the catalysts in dihydroxyacetone dehydration and pyruvaldehyde rehydration, we used pyruvaldehyde as a reactant. Our blank experiment showed a progressive increased pyruvaldehyde conversion with no observable lactic acid yield, which suggested that pyruvaldehyde thermally decomposed over time (Fig. 3). Z-900 gave the highest lactic acid yield of 50 % after 6 h. Interestingly, the lactic acid yield profiles of Z-500 (low LAS) and Z-900 (high LAS) with pyruvaldehyde as a reactant were similar to the yield profiles with dihydroxyacetone as a reactant (Fig. 2). These results suggested that dihydroxyacetone dehydration to pyruvaldehyde was a thermal reaction, whereas pyruvaldehyde rehydration to lactic acid was acid-catalyzed. Importantly, the LAS density controlled the pyruvaldehyde rehydration activity.

To further confirm the importance of LAS for pyruvaldehyde rehydration, we performed pyruvaldehyde rehydration with the acid-washed Z-900 (Z-900AW). Acid washing removed the EFAL species, sources of LAS, without modifying the porous properties of zeolites [60]. The Z-900AW catalyst showed a weak DRIFT band of adsorbed pyridine (1145 cm^{-1}) (**Fig. S5**), which suggested that most LAS of Z-900AW were removed after acid-wash. The pyruvaldehyde conversion and lactic acid yield profiles of Z-900AW were similar to the profiles of Z-500.

We further characterized spent catalysts by thermal gravimetric analysis (TGA) and differential thermogravimetry (DTG) to determine their deactivation mechanism related to acid site characteristics. Based on the TGA and DTG profiles, we observed the final weight loss in the order of Z-500 > Z-700 > Z-900. These weight loss values from spent catalysts were attributed to the formation of unwanted carbonaceous deposits, i.e., coke. These results suggested that Z-500 formed the highest amount of coke. This order was consistent with the abundance of

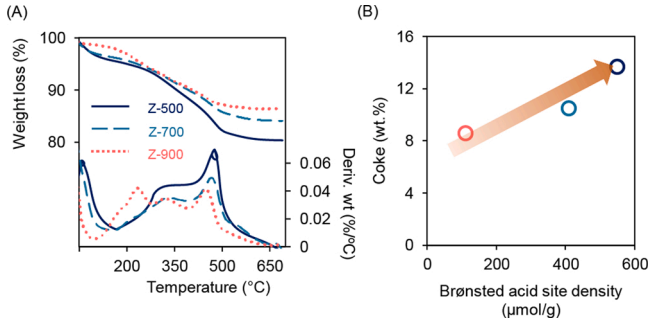

Fig. 4. TGA and DTG profiles of the spent catalysts (A) and the relationship between coke formation and Brønsted acid site density (B).

BAS (Fig. 4B). These results indicated that BAS was responsible for the formation of coke.

To determine the stability of lactic acid, we heated lactic acid at 140 °C for 6 h without catalyst (blank) and with catalysts, Z-500 and Z-900. Lactic acid conversion was <10 % in all cases (**Fig. S6**); thus, lactic acid was thermally stable under this experimental condition. Moreover, these results suggested that the catalysts did not cause side reactions with lactic acid.

4. Discussion

We investigated a heat treatment strategy to generate active Lewis acid sites (LAS) within ZSM-5. These LAS were active sites for dihydroxyacetone isomerization in water. The dihydroxyacetone isomerization reaction is a cascade of (1) dihydroxyacetone dehydration to pyruvaldehyde, followed by (2) pyruvaldehyde rehydration to lactic acid. Specifically, our results demonstrated that the dihydroxyacetone dehydration step was driven by reaction temperature, and the LAS were needed for pyruvaldehyde rehydration to lactic acid. Previously, little was known about the activities of the different acid sites in the reaction.

One of our most significant findings was that the high temperature treatment drove the modified ZSM-5 toward a high lactic acid selectivity. The heat treated ZSM-5 had a high LAS density. The dihydroxyacetone dehydration to pyruvaldehyde was a thermal reaction and pyruvaldehyde was formed readily at 140 °C, whereas LAS were needed to convert the resulting pyruvaldehyde to lactic acid. Moreover, the amount of LAS was consistent with the order of the catalytic performance, which suggested that the LAS were the active sites for pyruvaldehyde rehydration. Dapsens et al. [35] showed that an increase in LAS density by desilication of MFI zeolites enhanced the lactic acid selectivity of dihydroxyacetone conversion at 140 °C for 6 h. After acid washing, the LAS density of the desilicated MFI decreased, resulting in a decrease in the lactic acid. Takagaki et al. [54] used supported chromium and titanium oxide catalysts with varying compositions to generate catalysts with various LAS/BAS ratios for dihydroxyacetone conversion. They found that catalysts with a high LAS were more selective toward LA than those with low LAS. Our results agree with the findings of Dapsens et al. [35] and Takagaki et al. [54]

Another significant finding was that BAS did not have any activity in dihydroxyacetone isomerization. Moreover, the presence of BAS caused unwanted coke formation from pyruvaldehyde decomposition under our experimental condition (140 °C). The spent catalyst with high BAS (Z-500) had more coke compared to catalysts treated at 900 °C (Z-900). Takagaki et al. [54] showed that the presence of BAS in catalysts lowered the LA selectivity, results that corroborate our findings. Similarly, Nakajima et al. [58] used a Brønsted acid catalyst, H_2SO_4, for dihydroxyacetone isomerization and pyruvaldehyde rehydration. They did not observe any lactic acid yield at 100 °C, a further confirmation of our findings.

In comparing blank controls of dihydroxyacetone isomerization and pyruvaldehyde rehydration, we found that the blank control of dihydroxyacetone isomerization produced pyruvaldehyde as the only product, whereas the blank control of pyruvaldehyde rehydration did not produce any observable products. These results suggested that dihydroxyacetone dehydration to pyruvaldehyde was a thermal conversion and LAS was needed to convert pyruvaldehyde to lactic acid. Considering together the effects of reaction temperature, LAS, and BAS, we propose the chemical pathway of the modified ZSM-5 for dihydroxyacetone isomerization shown in Fig. 5. Dihydroxyacetone dehydration to pyruvaldehyde proceeded with reaction temperature (140 °C). The LAS generated within modified ZSM-5 was responsible for the selective dihydroxyacetone isomerization to lactic acid.

We summarized the performance of selected catalysts for dihydroxyacetone isomerization. West et al. compared the catalytic performance of different zeolites with different Si/Al ratios. They found that all zeolites were active in dihydroxyacetone isomerization, and the LA

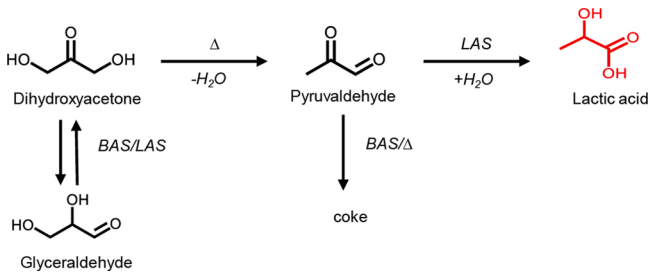

Fig. 5. Proposed chemical pathway for the dihydroxyacetone conversion to lactic acid by thermally treated ZSM-5. LAS = Lewis acid sites, BAS = Brønsted acid sites, Δ = heat.

selectivity was in the following order: H-USY (Si/Al = 6) > H-β (Si/Al = 12.5) > H-MOR (Si/Al = 10) > H-ZSM-5 (Si/Al = 11.5). Moreover, the zeolite with a low Si/Al ratio was more selective to lactic acid, and H-USY (Si/Al = 6) was the most selective to lactic acid (71 % lactic acid selectivity) (**Table S2**). Although these zeolites were active for dihydroxyacetone isomerization, their catalytic performance was still inferior to the Sn-based catalysts (Sn-containing β-zeolites [61,62] and Sn-containing silica [63]) with a high selectivity (>90 %) to lactic acid at a full conversion (**Table S3**). Two major limitations of using Sn-based catalysts are (1) a long and complicated synthesis [35], and (2) a scarcity of tin [64].

Clear advantages of this heat treatment approach are (1) the applicability to commercially available ZSM-5, and (2) the ability to control the LAS and BAS densities of ZSM-5 is a superior property compared with the active Sn-containing catalysts for dihydroxyacetone isomerization. Moreover, this strategy can be used for other acid-catalyzed reactions, such as dehydration [65], esterification [66], isomerization [67], etherification [68], and cascade reactions in which both LAS and BAS are needed, such as hydroxymethylfurfural production from cellulose [69,70]. The proximity of EFAL and Brønsted acid sites can lead to enhance catalytic activity of alkane cracking [71,72]. The enhancement of catalytic activity depends on the EFAL properties, such as proximity of EFAL concentration, speciation, location in the framework, distribution, and proximity of Bronsted acid sites [73]. Our work could be extended by identifying the EFAL features using ^{29}Si and ^{27}Al magic angle spinning nuclear magnetic resonance (MAS-NMR) spectroscopy in combination with density functional theory calculations [74,75] and correlating the results of MAS-NMR and density functional theory with catalytic activity. This information will be important for the development of a cost-effective and sustainable catalytic process for lactic acid production from biomass. In addition, the recyclability and change in mechanical property after catalyst recycling should be assessed to ensure long catalyst lifetime.

5. Conclusion

We investigated dihydroxyacetone isomerization in water using heat treated ZSM-5. The treatment at elevated temperature increased the Lewis acid sites density and decreased Brønsted acid site density of modified ZSM-5, which promoted high lactic acid selectivity in water. Dihydroxyacetone isomerization to lactic acid is a cascade of dehydration to pyruvaldehyde, followed by pyruvaldehyde rehydration to lactic acid. We demonstrated that dihydroxyacetone dehydration to pyruvaldehyde readily occurred at 140 °C and reached 50 % lactic acid yield after 6 h using heat treated ZSM-5 at 900 °C. The high LAS density of heat treated ZSM-5 was responsible for the pyruvaldehyde rehydration. This heat treatment strategy offers a new basis to tune LAS density for biomass processing reactions, including isomerization, dehydration, and esterification.

CRediT authorship contribution statement

Md Anwar Hossain: Conceptualization, Methodology, Validation, Investigation, Writing - original draft, Visualization. **Kyle N. Mills:** Investigation. **Ashten M. Molley:** Investigation. **Mohammad Shahinur Rahaman:** Investigation. **Sarttrawut Tulaphol:** Validation, Visualization. **Shashi B. Lalvani:** Writing - review & editing, Supervision. **Jie Dong:** Writing - review & editing, Supervision. **Mahendra K. Sunkara:** Writing - review & editing, Supervision, Funding acquisition. **Noppadon Sathitsuksanoh:** Conceptualization, Writing - original draft, Writing - review & editing, Supervision, Funding acquisition.

Declaration of Competing Interest

The authors report no declarations of interest.

Acknowledgement

A part of this material is based upon work supported by the National Science Foundation under Cooperative Agreement No. 1355438 and Internal Research Grant, Office of the Executive Vice President for Research, University of Louisville. This work was performed in part at the Conn Center for Renewable Energy Research at the University of Louisville, which belongs to the National Science Foundation NNCI KY Manufacturing and Nano Integration Node, supported by ECCS-1542174. The authors would like to thank Dr. Howard Fried for his valuable comments and suggestions on the manuscript.

Appendix A. Supplementary data

Supplementary material related to this article can be found, in the online version, at doi:https://doi.org/10.1016/j.apcata.2020.117979.

References

[1] Q. Zhang, J. Chang, T. Wang, Y. Xu, Energy Convers. Manage. 48 (2007) 87–92.
[2] S.N. Naik, V.V. Goud, P.K. Rout, A.K. Dalai, Renew. Sustain. Energy Rev. 14 (2010) 578–597.
[3] R. Datta, M. Henry, J. Chem. Technol. Biotechnol. 81 (2006) 1119–1129.
[4] O. Martin, L. Avérous, Polymer 42 (2001) 6209–6219.
[5] A. Repa, C. Grangette, C. Daniel, R. Hochreiter, K. Hoffmann-Sommergruber, J. Thalhamer, D. Kraft, H. Breiteneder, A. Mercenier, U. Wiedermann, Vaccine 22 (2003) 87–95.
[6] E. Zannini, D.M. Waters, A. Coffey, E.K. Arendt, Appl. Microbiol. Biotechnol. 100 (2016) 1121–1135.
[7] E. Vink, D. Glassner, J. Kolstad, R. Wooley, R. O'Connor, Ind. Biotechnol. 3 (2007) 58–81.
[8] C. Pereira, V. Silva, A. Rodrigues, Green Chem. 13 (2011) 2658–2671.
[9] K. Sakai, Y. Murata, H. Yamazumi, Y. Tau, M. Mori, M. Moriguchi, Y. Shirai, Food Sci. Technol. Res. 6 (2007) 140–145.
[10] E. Papamanoli, N. Tzanetakis, E. Litopoulou-Tzanetaki, P. Kotzekidou, Meat Sci. 65 (2003) 859–867.
[11] Y. Koito, K. Nakajima, M. Kitano, M. Hara, Chem. Lett. 42 (2013) 873–875.
[12] S. Lux, M. Siebenhofer, Chem. Biochem. Eng. Q. 29 (2015) 575–585.
[13] C.B. Rasrendra, B.A. Fachri, I.G.B. Makertihartha, S. Adisasmito, H.J. Heeres, ChemSusChem 4 (2011) 768–777.
[14] J. Cejka, A. Corma, S. Zones, Zeolites and Catalysis: Synthesis, Reactions and Applications, John Wiley & Sons, 2010.
[15] A. Martínez, G. Prieto, Top. Catal. 52 (2009) 75.
[16] A. Corma, Application of Zeolites in Fluid Catalytic Cracking and Related Processes, Studies in Surface Science and Catalysis, Elsevier, 1989, pp. 49–67.
[17] G. Caeiro, R. Carvalho, X. Wang, M. Lemos, F. Lemos, M. Guisnet, F.R. Ribeiro, J. Mol. Catal. A Chem. 255 (2006) 131–158.
[18] M.N. Akhtar, N. Al-Yassir, S. Al-Khattaf, J. Čejka, Catal. Today 179 (2012) 61–72.
[19] A. Smiešková, E. Rojasová, P. Hudec, L. Šabo, Appl. Catal. A Gen. 268 (2004) 235–240.
[20] M.S. Rahaman, T.K. Phung, M.A. Hossain, E. Chowdhury, S. Tulaphol, S.B. Lalvani, M. O'Toole, G.A. Willing, J.B. Jasinski, M. Crocker, Appl. Catal. A Gen. (2020), 117369.
[21] C. Patil, P. Niphadkar, V. Bokade, P. Joshi, Catal. Commun. 43 (2014) 188–191.
[22] P. Ferreira, I. Fonseca, A. Ramos, J. Vital, J. Castanheiro, Catal. Commun. 10 (2009) 481–484.
[23] S.R. Kirumakki, N. Nagaraju, K.V. Chary, S. Narayanan, Appl. Catal. A Gen. 248 (2003) 161–167.
[24] S.R. Kirumakki, N. Nagaraju, S. Narayanan, Appl. Catal. A Gen. 273 (2004) 1–9.
[25] S.R. Kirumakki, N. Nagaraju, K.V. Chary, Appl. Catal. A Gen. 299 (2006) 185–192.
[26] L. Young, S. Butter, W. Kaeding, J. Catal. 76 (1982) 418–432.
[27] V.R. Choudhary, S.K. Jana, B. Kiran, Catal. Letters 59 (1999) 217–219.
[28] A. Palomares, G. Eder-Mirth, J. Lercher, J. Catal. 168 (1997) 442–449.
[29] M. Moliner, Y. Román-Leshkov, M.E. Davis, Proc. Natl. Acad. Sci. 107 (2010) 6164–6168.
[30] R. Bermejo-Deval, R.S. Assary, E. Nikolla, M. Moliner, Y. Román-Leshkov, S.-J. Hwang, A. Palsdottir, D. Silverman, R.F. Lobo, L.A. Curtiss, Proc. Natl. Acad. Sci. 109 (2012) 9727–9732.
[31] T. Isoda, S. Nagao, X. Ma, Y. Korai, I. Mochida, Energy Fuels 10 (1996) 1078–1082.
[32] X. Wang, F. Liang, C. Huang, Y. Li, B. Chen, Catal. Sci. Technol. 5 (2015) 4410–4421.
[33] J. Wang, Y. Masui, M. Onaka, Appl. Catal. B 107 (2011) 135–139.
[34] Q. Guo, F. Fan, E.A. Pidko, W.N. Van Der Graaff, Z. Feng, C. Li, E.J. Hensen, ChemSusChem 6 (2013) 1352–1356.
[35] P.Y. Dapsens, C. Mondelli, J. Pérez-Ramírez, ChemSusChem 6 (2013) 831–839.
[36] J. van Bokhoven, M. Tromp, D. Koningsberger, J. Miller, J. Pieterse, J. Lercher, B. Williams, H. Kung, J. Catal. 202 (2001) 129–140.
[37] A. To, R. Jentoft, W. Alvarez, S. Crossley, D. Resasco, J. Catal. 317 (2014) 11–21.
[38] T. Hoff, R. Thilakaratne, D. Gardner, R. Brown, J.-P. Tessonnier, J. Phys. Chem. C 120 (2016) 20103–20113.
[39] P.P. Pescarmona, K.P.F. Janssen, C. Delaet, C. Stroobants, K. Houthoofd, A. Philippaerts, C. De Jonghe, J.S. Paul, P.A. Jacobs, B.F. Sels, Green Chem. 12 (2010) 1083–1089.
[40] Y. Chu, X. Yi, C. Li, X. Sun, A. Zheng, Chem. Sci. 9 (2018) 6470–6479.
[41] T.C. Hoff, R. Thilakaratne, D.W. Gardner, R.C. Brown, J. Tessonnier, J. Phys. Chem. C 120 (2016) 20103–20113.
[42] S. Brunauer, P. Emmett, E. Teller, J. Am. Chem. Soc. 60 (1938) 309–319.
[43] E. Barrett, L. Joyner, P. Halenda, J. Am. Chem. Soc. 73 (1951) 373–380.
[44] Y. Ji, A. Lawal, A. Nyholm, R. Gorte, O. Abdelrahman, Catal. Sci. Technol. (2020).
[45] F. Jin, Y. Li, Catal. Today 145 (2009) 101–107.
[46] J. Rorrer, Y. He, F.D. Toste, A.T. Bell, J. Catal. 354 (2017) 13–23.
[47] A. Starace, B. Black, D. Lee, E. Palmiotti, K. Orton, W. Michener, J. ten Dam, M. Watson, G. Beckham, K. Magrini, C. Mukarakate, ACS Sustain. Chem. Eng. 5 (2017) 11761–11769.
[48] M. Rutkowska, D. Macina, Z. Piwowarska, M. Gajewska, U. Díaz, L. Chmielarz, Catal. Sci. Technol. 6 (2016) 4849–4862.
[49] H. Van Koningsveld, J. Jansen, H. Van Bekkum, Zeolites 10 (1990) 235–242.
[50] C. Triantafillidis, A. Vlessidis, L. Nalbandian, N. Evmiridis, Microporous Mesoporous Mater. 47 (2001) 369–388.
[51] K.S. Triantafyllidis, L. Nalbandian, P.N. Trikalitis, A.K. Ladavos, T. Mavromoustakos, C.P. Nicolaides, Microporous Mesoporous Mater. 75 (2004) 89–100.
[52] S. Li, A. Zheng, Y. Su, H. Zhang, L. Chen, J. Yang, C. Ye, F. Deng, J. Am. Chem. Soc. 129 (2007) 11161–11171.
[53] R. Shannon, K. Gardner, R. Staley, G. Bergeret, P. Gallezot, A. Auroux, J. Phys. Chem. 89 (1985) 4778–4788.
[54] A. Takagaki, H. Goto, R. Kikuchi, S. Oyama, Appl. Catal. A 570 (2019) 200–208.
[55] E. Jolimaitre, D. Delcroix, N. Essayem, C. Pinel, M. Besson, Catal. Sci. Technol. 8 (2018) 1349–1356.
[56] X. Wang, F. Liang, C. Huang, Y. Li, B. Chen, Catal. Sci. Technol. 6 (2016) 6551–6560.
[57] R.M. West, M.S. Holm, S. Saravanamurugan, J. Xiong, Z. Beversdorf, E. Taarning, C.H. Christensen, J. Catal. 269 (2010) 122–130.
[58] K. Nakajima, J. Hirata, M. Kim, N. Gupta, T. Murayama, A. Yoshida, N. Hiyoshi, A. Fukuoka, W. Ueda, ACS Catal. 8 (2018) 283–290.
[59] K. Santos, E. Albuquerque, L. Borges, M. Fraga, Mol. Catal. 458 (2018) 198–205.
[60] D. Verboekend, A. Chabaneix, K. Thomas, J.-P. Gilson, J. Pérez-Ramírez, CrystEngComm 13 (2011) 3408–3416.
[61] A. Feliczak-Guzik, M. Sprynskyy, I. Nowak, B. Buszewski, Catalysts 8 (2018) 31.
[62] E. Taarning, S. Saravanamurugan, M. Holm, J. Xiong, R. West, C. Christensen, ChemSusChem 2 (2009) 625–627.
[63] X. Wang, F. Liang, C. Huang, Y. Li, B. Chen, Catal. Sci. Technol. 6 (2016) 6551–6560.
[64] P. Smith, Chemistry of Tin, Springer Science & Business Media, 2012.
[65] K.A. Tarach, J. Tekla, U. Filek, A. Szymocha, I. Tarach, K. Góra-Marek, Microporous Mesoporous Mater. 241 (2017) 132–144.
[66] D.M. Dal Pozzo, J.A. Azevedo dos Santos, E.S. Júnior, R.F. Santos, A. Feiden, S. N. Melegari de Souza, I. Burgardt, RSC Adv. 9 (2019) 4900–4907.
[67] A.P. Bolton, M.A. Lanewala, J. Catal. 18 (1970) 1–11.
[68] P.M. Veiga, A.C.L. Gomes, C.O. Veloso, C.A. Henriques, Appl. Catal. A Gen. 548 (2017) 2–15.
[69] F. Yang, J. Fu, J. Mo, X. Lu, Energy Fuels 27 (2013) 6973–6978.
[70] S. Tulaphol, M.A. Hossain, M.S. Rahaman, L.Y. Liu, T.K. Phung, S. Renneckar, N. Grisdanurak, N. Sathitsuksanoh, Energy Fuels 34 (2020) 1764–1772.
[71] N. Xue, A. Vjunov, S. Schallmoser, J. Fulton, M. Sanchez-Sanchez, J. Hu, D. Mei, J. Lercher, J. Catal. 365 (2018) 359–366.
[72] R. Gounder, A. Jones, R. Carr, E. Iglesia, J. Catal. 286 (2012) 214–223.
[73] T. Le, A. Chawla, J. Rimer, J. Catal. (2020).
[74] X. Yi, K. Liu, W. Chen, J. Li, S. Xu, C. Li, Y. Xiao, H. Liu, X. Guo, S.-B. Liu, A. Zheng, JACS 140 (2018) 10764–10774.
[75] A. Zheng, S. Li, S.-B. Liu, F. Deng, Acc. Chem. Res. 49 (2016) 655–663.